

# Approximate Partially Decentralized Linear EZF Precoding for Massive MU-MIMO Systems

Brikena Kaziu<sup>1</sup>, Nikita Shanin<sup>1</sup>, Danilo Spano<sup>2</sup>, Li Wang<sup>2</sup>, Wolfgang Gerstacker<sup>1</sup>, and Robert Schober<sup>1</sup>

<sup>1</sup>Friedrich-Alexander-Universität (FAU) Erlangen-Nürnberg,

<sup>2</sup>Huawei Technologies Sweden AB

**Abstract**—Massive multi-user multiple-input multiple-output (MU-MIMO) systems enable high spatial resolution, high spectral efficiency, and improved link reliability compared to traditional MIMO systems due to the large number of antenna elements deployed at the base station (BS). Nevertheless, conventional massive MU-MIMO BS transceiver designs rely on centralized linear precoding algorithms, which entail high interconnect data rates and a prohibitive complexity at the centralized baseband processing unit. In this paper, we consider an MU-MIMO system, where each user device is served with multiple independent data streams in the downlink. To address the aforementioned challenges, we propose a novel decentralized BS architecture, and develop a novel decentralized precoding algorithm based on eigen-zero-forcing (EZF). Our proposed approach relies on parallelizing the baseband processing tasks across multiple antenna clusters at the BS, while minimizing the interconnection requirements between the clusters, and is shown to closely approach the performance of centralized EZF.

## I. INTRODUCTION

Massive multiple-input multiple-output (MIMO) systems are an extension of traditional MIMO communication systems, where hundreds or even thousands of active antenna elements are deployed at the base station (BS) and a large number of user terminals is served simultaneously [1]–[4]. The main advantages of massive MIMO systems compared to traditional MIMO are a higher spatial resolution, higher spectral efficiency, improved link reliability, and lower latency [2], [3]. Despite the prominence of massive MIMO, the large number of antenna elements at the BS results also in several implementation challenges [1], [2], [5]. In particular, conventional baseband signal processing algorithms that fully exploit the potential of massive MIMO systems, such as zero-forcing (ZF) [6] and eigen-zero-forcing (EZF) [7] precoding for single-antenna and multi-antenna users, respectively, rely on a centralized BS architecture, see Fig. 1. As shown in Fig. 1, the central processing unit (CPU) estimates the channel state information (CSI) and computes a precoder in the *ChEst* and *Precoder* blocks, respectively. Additionally, the CPU applies the precoding weights to the transmit symbols, which are generated by the source  $S$ , and forwards the precoded symbols to the radio frequency (RF) chains. Therefore, for the centralized BS design in Fig. 1, the complete CSI and all transmit data streams have to be available at the CPU to perform all the baseband processing tasks in a centralized manner. This results in an excessively high amount of raw baseband data, i.e., fronthaul load, that must be exchanged between the CPU and the RF units via the *fronthaul bus* and increases the computational complexity at the CPU.

New distributed baseband processing architectures are proposed in [8]–[11], where the antennas at the BS are grouped into

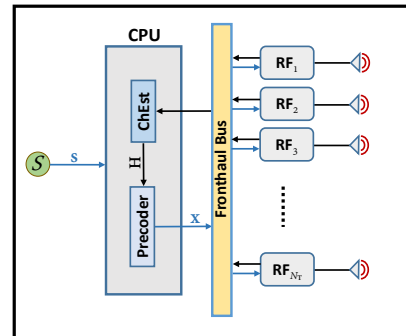


Fig. 1: Centralized BS architecture with  $N_T$  antennas connected via a shared fronthaul bus to a CPU.

clusters and equipped with their own circuitry and hardware, facilitating decentralized baseband signal processing. Furthermore, each BS cluster locally estimates the corresponding local CSI. In particular, to compute the local precoding vectors at the antenna clusters, the authors in [8] develop an algorithm, which is based on the alternating direction method of multipliers (ADMM), and relies on iterative consensus-information-sharing between the clusters via a fusion node. The authors in [9] propose a partially decentralized (PD) algorithm to compute the local precoding vectors at the BS clusters based on the Wiener filter and a feedforward architecture, which achieves exactly the same performance as the centralized counterpart, but with a lower fronthaul overhead. In [9], the antenna clusters send the Gram matrices computed based on the locally estimated channel matrices to a central node, where the Wiener filter precoding weights are computed. Furthermore, the authors in [9] also propose a fully decentralized (FD) approach, where each antenna cluster determines its local precoding weights using only its local CSI, without sharing any information with the other clusters. Since the FD architecture in [9] does not rely on any information exchange between the BS clusters, it experiences a significant performance loss compared to the PD precoding scheme. Based on the FD feedforward architecture in [9], a decentralized ZF precoding approach using the coordinate descent (CD) algorithm at each BS cluster is introduced in [10]. The authors in [11] propose a new BS topology referred to as daisy chain architecture, where the antenna units communicate with each other using unidirectional links, and execute the precoding procedure in a sequential fashion. An extension of this work is reported in [12], where a downlink precoding scheme based on the CD algorithm is presented. The results reveal that the required inter-connection data-rate is lower compared to the centralized ZF approach, however, at the expense of a

performance loss.

Although the decentralized iterative algorithms in [8], [10] achieve almost the same performance as their centralized counterparts, they compute the final precoded symbol vectors instead of the precoder matrices, and therefore, they have to be executed multiple times within a coherence block, making them impractical for systems with a large coherence time, see also [13]. Furthermore, for their analysis, the authors in [8]–[12] assume that the user devices are equipped with a single antenna and the system load, i.e., the ratio of the total number of users to the total number of antennas at the BS, is lower than 25%, which is an assumption that does not always hold for massive MIMO systems in practice [4].

To account for systems with multiple-antenna user devices, the authors in [14] show that the mathematical operations of the EZF scheme can be distributed among the BS clusters, and thus, the EZF precoding vectors can be computed efficiently with a lower fronthaul overhead, while achieving exactly the same performance as the centralized approach. However, the fronthaul load and per-node computational complexities of the decentralized EZF (DEZF) approach in [14] may still be too high for a practical implementation if the number of BS clusters and the number of user devices are high. Therefore, we aim at designing a PD BS architecture and a linear signal precoding scheme that yield a further fronthaul load and per-node complexity reduction at the BS.

To this end, in this paper, we consider a downlink massive multi-user MIMO (MU-MIMO) system, where the user devices are equipped with multiple antennas and served with multiple data streams. The main contributions of this work are summarized as follows. Motivated by the PD architectures in [8]–[10], [14], we propose and analyze a novel distributed architecture for massive MU-MIMO BSs. In contrast to the BS architectures in [8]–[10], [14], the proposed BS design does not rely on a CPU node, but the computational complexity burden of the baseband signal processing tasks is distributed across different clusters of BS antennas. Moreover, for the proposed BS architecture, we develop a novel approximate partially decentralized (APD) precoding scheme based on the EZF precoding algorithms in [7], [14]. We demonstrate that the proposed APD approach yields lower fronthaul and per-node computational complexities than the centralized scheme and the DEZF scheme in [7] and [14], respectively. Furthermore, our numerical results indicate that the proposed distributed signal processing scheme closely approaches the performance of centralized EZF.

The remainder of the paper is organized as follows. In Section II, we introduce the downlink system model and the baseline centralized EZF precoding scheme. In Section III, we propose a novel distributed BS architecture and the APD precoding scheme. In Section IV, we analyze the fronthaul load generated at the BS for the centralized BS architecture with centralized EZF precoding, the proposed decentralized BS architecture with APD EZF precoding, and the DEZF approach. Furthermore, we numerically evaluate the performance of the proposed scheme and compare the obtained results with the performance of the centralized EZF, DEZF, and FD EZF precoding schemes.

Section V concludes this paper.

*Notations:* Boldface capital letters  $\mathbf{A}$  and boldface lower case letters  $\mathbf{a}$  denote matrices and vectors, respectively.  $A_{i,j}$  stands for the element in the  $i$ th row and  $j$ th column of matrix  $\mathbf{A}$ , whereas  $a_i$  is the  $i$ th element of vector  $\mathbf{a}$ .  $\mathbf{A}^T$ ,  $\mathbf{A}^H$ , and  $\text{tr}(\mathbf{A})$  denote the transpose, Hermitian transpose, and trace of matrix  $\mathbf{A}$ , respectively. The Euclidean norm of vector  $\mathbf{a}$  and the induced Euclidean norm of matrix  $\mathbf{A}$  are represented by  $\|\mathbf{a}\|$  and  $\|\mathbf{A}\|$ , respectively. Furthermore,  $\mathbf{A}^\dagger$  denotes the Moore-Penrose pseudo-inverse of matrix  $\mathbf{A}$ .  $\mathbb{C}^{m \times n}$  is the set of all  $m \times n$  matrices with complex-valued entries and  $\mathbf{I}_N$  denotes the  $N \times N$  identity matrix.  $\text{Blkdiag}\{\mathbf{A}_1, \dots, \mathbf{A}_K\}$  denotes a block diagonal matrix, whose block diagonal entries are  $\mathbf{A}_1, \dots, \mathbf{A}_K$ , whereas  $\text{diag}\{\mathbf{A}\}$  extracts the main diagonal entries of a matrix  $\mathbf{A}$  to a vector. Statistical expectation is represented by  $\mathbb{E}\{\cdot\}$ .

## II. DOWNLINK SYSTEM MODEL AND CENTRALIZED PRECODING

In this section, we introduce the considered MU-MIMO downlink system model and discuss the centralized EZF precoding scheme.

### A. Downlink System Model

We consider a single-cell downlink MU-MIMO system comprising a BS equipped with  $N_T \geq 1$  antennas and  $K \geq 1$  user devices. Each user is equipped with  $N_R \geq 1$  antennas and is simultaneously served by the BS with  $L \leq N_R$  independent data streams. Thus, the total number of independent data streams broadcast by the BS is given by  $L_{\text{tot}} = KL \leq N_T$ . We assume time division duplex (TDD) transmission, where channel reciprocity holds. At the beginning of each transmission time interval, the BS computes linear precoding vectors based on the uplink CSI. Throughout this paper, we assume that perfect CSI<sup>1</sup> of all downlink channels is available at the BS, whereas each user device has access only to its own CSI. The precoding vectors are then applied to the data transmitted to the user devices in the downlink.

The received complex baseband signal at user  $k$ ,  $k = \{1, 2, \dots, K\}$ , can be expressed as follows:

$$\mathbf{y}_k = \sqrt{\gamma} \mathbf{H}_k \mathbf{W} \mathbf{s} + \mathbf{n}_k, \quad (1)$$

where  $\mathbf{W} \in \mathbb{C}^{N_T \times L_{\text{tot}}}$  is the linear precoding matrix at the BS,  $\mathbf{H}_k \in \mathbb{C}^{N_R \times N_T}$  is the overall downlink channel of user  $k$ , and  $\mathbf{n}_k \in \mathbb{C}^{N_R \times 1}$  denotes the additive white Gaussian noise (AWGN) at user  $k$ ,  $\forall k$ , with zero mean and covariance matrix  $\sigma_n^2 \mathbf{I}_{N_R}$ . The independent transmit symbols collected in vector  $\mathbf{s} = [s_1 \dots s_{L_{\text{tot}}}]^T \in \mathcal{M}^{L_{\text{tot}}}$ , where  $\mathcal{M}$  is the symbol constellation set of the adopted linear modulation scheme, are generated at the source block  $S$  of the BS, cf. Fig. 1. Without loss of generality, in this paper, we assume equal power distribution across all users and transmit data streams. The transmit power loading factor  $\gamma$  in (1) is chosen according to  $\mathbb{E}\{\|\sqrt{\gamma} \mathbf{W} \mathbf{s}\|^2\} = P_{\text{BS}}$ , where  $P_{\text{BS}}$  is the total power constraint at the BS.

<sup>1</sup>In this work, we aim at obtaining an upper bound for the system performance, and therefore, we neglect the impact of imperfect CSI.

To detect the current information symbol of its data stream  $l$ ,  $l = \{1, 2, \dots, L\}$ , user  $k$ ,  $\forall k$ , multiplies the received vector  $\mathbf{y}_k$  by the equalization vector  $\mathbf{f}_{k,l} \in \mathbb{C}^{N_R \times 1}$  as follows:

$$\begin{aligned} r_{k,l} &= \mathbf{f}_{k,l}^H \mathbf{y}_k = \sqrt{\gamma} \mathbf{f}_{k,l}^H \mathbf{H}_k \mathbf{W} \mathbf{s} + \mathbf{f}_{k,l}^H \mathbf{n}_k \\ &= \sqrt{\gamma} \mathbf{c}_{k,l} \mathbf{x} + \tilde{n}_{k,l}, \end{aligned} \quad (2)$$

where  $\mathbf{x} = \mathbf{W} \mathbf{s} \in \mathbb{C}^{N_T \times 1}$  is the precoded transmit vector, and  $\mathbf{c}_{k,l} = \mathbf{f}_{k,l}^H \mathbf{H}_k \in \mathbb{C}^{1 \times N_T}$  and  $\tilde{n}_{k,l}$  are the equivalent channel vector and the additive Gaussian noise effective after equalization of stream  $l$  at user  $k$ ,  $\forall k, l$ , respectively. Since we assume perfect CSI knowledge at the BS and the user devices, user  $k$  and the BS can compute both the same vector  $\mathbf{f}_{k,l}$ ,  $\forall k, l$ . Finally, vector  $\mathbf{r} = [r_{1,1} \ r_{1,2} \ \dots \ r_{k,l} \ \dots \ r_{K,L}]^T \in \mathbb{C}^{L_{\text{tot}} \times 1}$  collecting the equalized data streams of all user devices can be expressed as follows:

$$\mathbf{r} = \sqrt{\gamma} \mathbf{C} \mathbf{W} \mathbf{s} + \tilde{\mathbf{n}} = \sqrt{\gamma} \mathbf{C} \mathbf{x} + \tilde{\mathbf{n}}, \quad (3)$$

where  $\mathbf{C} = [\mathbf{c}_{1,1}^T \ \mathbf{c}_{1,2}^T \ \dots \ \mathbf{c}_{k,l}^T \ \dots \ \mathbf{c}_{K,L}^T]^T \in \mathbb{C}^{L_{\text{tot}} \times N_T}$  is the equivalent composite downlink channel, and  $\tilde{\mathbf{n}} = [\tilde{n}_{1,1} \ \tilde{n}_{1,2} \ \dots \ \tilde{n}_{k,l} \ \dots \ \tilde{n}_{K,L}]^T \in \mathbb{C}^{L_{\text{tot}} \times 1}$ .

### B. Centralized EZF Precoding

In the following, we present the linear EZF precoding scheme. In addition to performing perfect interference cancellation between different data streams and user devices, linear EZF precoding also steers the transmit vector to align with the direction in which the user experiences maximum gain, i.e., where the user has the strongest channel, [7], [14]. The optimum direction is determined based on the singular value decomposition (SVD) of the channel matrix of each user [7], [14], [15]. To this end, let us first define the SVD of channel matrix  $\mathbf{H}_k$ ,  $\forall k$ , as  $\mathbf{H}_k = \mathbf{U}_k \mathbf{\Lambda}_k \mathbf{V}_k^H$ , where  $\mathbf{\Lambda}_k \in \mathbb{C}^{N_R \times N_T}$  is a diagonal matrix containing the singular values of  $\mathbf{H}_k$ , i.e.,  $\lambda_{k,j}$ ,  $j = \{1, 2, \dots, N_R\}$ , in a decreasing order along its main diagonal. Here,  $\mathbf{U}_k = [\mathbf{u}_{k,1} \ \mathbf{u}_{k,2} \ \dots \ \mathbf{u}_{k,N_R}] \in \mathbb{C}^{N_R \times N_R}$  and  $\mathbf{V}_k = [\mathbf{v}_{k,1} \ \mathbf{v}_{k,2} \ \dots \ \mathbf{v}_{k,N_T}] \in \mathbb{C}^{N_T \times N_T}$  are unitary matrices, where  $\mathbf{u}_{k,j}$  and  $\mathbf{v}_{k,j}$  are the left and right singular vectors of matrix  $\mathbf{H}_k$ , respectively, which correspond to the  $j$ th largest singular value  $\lambda_{k,j}$ ,  $\forall k, j$ .

To detect the  $l$ th data stream,  $l = \{1, 2, \dots, L\}$ , at user  $k$ ,  $\forall k$ , the equalization vector  $\mathbf{f}_{k,l}$  is chosen by the CPU as  $\mathbf{f}_{k,l} = \mathbf{u}_{k,l}$  [7]. Thus, the equivalent channel vector of stream  $l$  and user  $k$  can be expressed as  $\mathbf{c}_{k,l} = \mathbf{u}_{k,l}^H \mathbf{H}_k$ ,  $\forall k, l$ . Then, we determine the precoding matrix  $\mathbf{W} = [\mathbf{w}_1 \ \mathbf{w}_2 \ \dots \ \mathbf{w}_{L_{\text{tot}}}]$ , where  $\mathbf{w}_i$  is the precoding vector for the  $i$ th data stream,  $i = \{1, \dots, L_{\text{tot}}\}$ , defined as  $\mathbf{w}_i = \frac{\hat{\mathbf{c}}_i}{\|\hat{\mathbf{c}}_i\|}$ , where  $\hat{\mathbf{c}}_i$  is the  $i$ th column of matrix  $\mathbf{C}^\dagger = \mathbf{C}^H (\mathbf{C} \mathbf{C}^H)^{-1}$  [7]. Finally, the detected signal vector in (3) can be expressed as:

$$\mathbf{r} = \sqrt{\gamma} \tilde{\mathbf{s}} + \tilde{\mathbf{n}}, \quad (4)$$

where  $\tilde{\mathbf{s}} = [s_1 / \|\hat{\mathbf{c}}_1\| \ \dots \ s_{L_{\text{tot}}} / \|\hat{\mathbf{c}}_{L_{\text{tot}}}\|]^T$  is the desired (normalized) symbol vector.

We note that, for the BS architecture shown in Fig. 1, the computation of the EZF precoding vectors requires the full CSI to be available at the CPU. Furthermore, the precoded

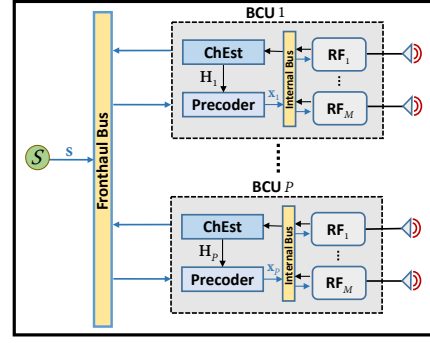


Fig. 2: Decentralized BS architecture, where the antennas are organized into  $P$  BCUs, which are connected via a shared fronthaul bus and perform local channel estimation and signal processing.

transmit signal vector  $\mathbf{x}$ , which scales with  $N_T$ , has to be forwarded from the CPU to the RF chains via the *fronthaul bus*, see Fig. 1, resulting in a high fronthaul load for large  $N_T$ . Moreover, the CPU carries the full computational burden making the centralized implementation of the EZF scheme infeasible for large numbers of BS antennas, since complex operations are performed with high-dimensional matrices [1], [2].

## III. PROPOSED DECENTRALIZED PRECODING

To alleviate the high fronthaul requirements and the high computational load of the centralized EZF scheme, in the following, we propose a novel distributed BS architecture and derive the APD EZF algorithm.

### A. Decentralized BS Architecture

In contrast to the centralized BS architecture depicted in Fig. 1, we propose a decentralized BS architecture as shown in Fig. 2. In particular, we partition the antennas employed at the BS into  $P \geq 1$  clusters, which we refer to as basic component units (BCUs). Each BCU is equipped with  $M$  antennas (i.e., we have  $PM = N_T$ ), and has its own *ChEst* and *Precoder* block for local CSI acquisition and local precoder computation, respectively. We note that in contrast to the BS architectures in [8]–[10], [14], our proposed BS design does not employ a CPU node for aggregated baseband signal processing. Furthermore, each BCU is connected via the fronthaul bus to the other BCUs, as shown in Fig. 2. Such an architecture enables a scalable BS design, where adding or removing antenna elements is equivalent to adding/removing BCUs.

We assume that the  $p$ th BCU has knowledge of only its own local baseband channel between the corresponding antennas and all deployed user devices. We denote the local channel matrix of BCU  $p$  as  $\mathbf{H}^p = [\mathbf{H}_{1,p}^T \ \mathbf{H}_{2,p}^T \ \dots \ \mathbf{H}_{K,p}^T]^T \in \mathbb{C}^{K N_R \times M}$ ,  $p = \{1, 2, \dots, P\}$ , where  $\mathbf{H}_{k,p}$  is the channel matrix between BCU  $p$  and user  $k$ ,  $k = \{1, \dots, K\}$ . Based on the estimated local channel matrix  $\mathbf{H}^p$  and the information received from the other BCUs, BCU  $p$  computes the local precoding matrix  $\mathbf{W}_p \in \mathbb{C}^{M \times L_{\text{tot}}}$ ,  $\forall p$ . We note that the complete precoding matrix at the BS can be represented as  $\mathbf{W} = [\mathbf{W}_1^T \ \mathbf{W}_2^T \ \dots \ \mathbf{W}_P^T]^T$ . Finally, similar to the centralized BS design in Fig. 1, we assume that

the data symbols in vector  $\mathbf{s}$  are generated at the source block  $S$  of the BS and transmitted to the BCUs at the beginning of each transmission time interval, via the *fronthaul bus*, see Fig. 2.

### B. Approximate Partially-Decentralized EZF Precoding

In the following, we derive the APD EZF precoding scheme, which is based on the centralized EZF approach discussed in Section II-A and relies on the decentralized architecture depicted in Fig. 2.

First, let us define block diagonal matrix  $\mathbf{D} = \text{Blkdiag}\{\tilde{\mathbf{U}}_1^H \dots \tilde{\mathbf{U}}_K^H\} \in \mathbb{C}^{L_{\text{tot}} \times K N_{\text{R}}}$ , where  $\tilde{\mathbf{U}}_k = [\mathbf{u}_{k,1} \dots \mathbf{u}_{k,L}] \in \mathbb{C}^{N_{\text{R}} \times L}$  is the equalization matrix of user  $k$ ,  $k = \{1, 2, \dots, K\}$ . Next, the equivalent channel matrix  $\mathbf{C}$  can be expressed as follows:

$$\mathbf{C} = \mathbf{D}[\mathbf{H}^1 \dots \mathbf{H}^P] = [\mathbf{C}_1 \ \mathbf{C}_2 \ \dots \ \mathbf{C}_P], \quad (5)$$

where  $\mathbf{C}_p = \mathbf{D}\mathbf{H}^p$  is the local equivalent composite channel matrix of BCU  $p$ ,  $p = \{1, \dots, P\}$ . Then, we compute the Gram matrix  $\mathbf{G} = \mathbf{C}\mathbf{C}^H$  of the equivalent channel matrix as

$$\mathbf{G} = \sum_{p=1}^P \mathbf{D}\mathbf{H}^p(\mathbf{H}^p)^H\mathbf{D}^H = \sum_{p=1}^P \underbrace{\mathbf{C}_p\mathbf{C}_p^H}_{\mathbf{G}_p} = \sum_{p=1}^P \mathbf{G}_p. \quad (6)$$

Finally, the local precoding matrix can be obtained at BCU  $p$  as follows:

$$\mathbf{W}_p = [\mathbf{w}_{p,1} \dots \mathbf{w}_{p,L_{\text{tot}}}] = \mathbf{C}_p^H \mathbf{G}^{-1} \mathbf{Q}^{-\frac{1}{2}}, \quad \forall p, \quad (7)$$

where  $\mathbf{w}_{p,i}$  is the local precoding vector at BCU  $p$  for data stream  $i$ ,  $\forall p, i$ , and  $\mathbf{Q}$  is a diagonal matrix comprising the squared column norms of matrix  $\mathbf{C}^\dagger$  in the main diagonal, i.e.,  $\text{diag}\{\mathbf{Q}\} = \text{diag}\{(\mathbf{C}^\dagger)^H \mathbf{C}^\dagger\} = \text{diag}\{\mathbf{G}^{-1}\}$ . Similar to the EZF precoding vectors in Section II-B, the multiplication by  $\mathbf{Q}^{-\frac{1}{2}}$  ensures that the columns  $\mathbf{w}_i = [\mathbf{w}_{1,i}^T \dots \mathbf{w}_{P,i}^T]^T$ ,  $\forall i$ , of the derived composite precoder matrix  $\mathbf{W}$  have unit norm.

In order to obtain the local precoding matrices  $\mathbf{W}_p$ , the BCUs first need to compute matrix  $\mathbf{D}$ . To this end, as proposed in [14], the BCUs could share the Gram matrices of their local channel matrices  $\mathbf{H}_G^{k,p} = \mathbf{H}_{k,p} \mathbf{H}_{k,p}^H$ ,  $\forall k, p$ , and then, locally independently compute the SVD of the aggregate matrix  $\mathbf{H}_G = \sum_{p=1}^P \mathbf{H}_{k,p} \mathbf{H}_{k,p}^H$  to obtain the equalization vectors  $\mathbf{f}_{k,l}$ ,  $\forall k, l$ . However, this approach may yield a high fronthaul load for a large number of user devices  $K$ . Moreover, in this case, each BCU has to compute the SVDs of  $K$  aggregate Gram matrices, which may lead to undesirably high computational requirements at the BS. Therefore, to reduce the fronthaul load and the computational complexity of calculating the precoding vectors, in the following, we approximate matrix  $\mathbf{D}$ .

First, for each user  $k$ ,  $\forall k$ , we identify a *strongest* BCU, i.e., the BCU with the strongest channel to user  $k$ , that will lend itself for the computation of the equalization matrix of user  $k$ . To this end, we introduce the metric  $\mathcal{T}_{k,p} = \text{tr}(\mathbf{H}_G^{k,p})$ , which is computed at BCU  $p$ ,  $\forall p, k$ . Then, the BCUs share the locally computed metrics  $\mathcal{T}_{k,p}$ ,  $\forall p, k$ , via the *fronthaul bus* and each BCU identifies the *strongest* unit for each user device as follows:

$$p_k^* = \underset{p=\{1, \dots, P\}}{\text{argmax}} \mathcal{T}_{k,p}, \quad k = \{1, \dots, K\}. \quad (8)$$

Note that other metrics can be used to define the *strongest* BCU, e.g.,  $\|\mathbf{H}_{k,p}\|$ ,  $\forall k, p$ . Nevertheless, since Gram matrix  $\mathbf{H}_G^{k,p}$  has to be computed to obtain the block diagonal entries of matrix  $\mathbf{G}_p$ , cf. (6), we gain in computational efficiency by reusing its values for  $\mathcal{T}_{k,p}$ ,  $\forall k, p$ , unlike for other possible metrics. Finally, BCU  $p_k^*$  computes the equalization matrix of user  $k$  as  $\tilde{\mathbf{U}}_{k,p_k^*} = [\mathbf{u}_{k,1}^{p_k^*} \dots \mathbf{u}_{k,L}^{p_k^*}]$ , where  $\mathbf{u}_{k,l}^{p_k^*}$  is the  $l$ th dominant eigenvector of Gram matrix  $\mathbf{H}_G^{k,p_k^*} = \mathbf{H}_{k,p_k^*}(\mathbf{H}_{k,p_k^*})^H$ ,  $\forall k, l = \{1, \dots, L\}$ .

Next, the *strongest* BCU  $p_k^*$  for user  $k$ , broadcasts the locally obtained  $\tilde{\mathbf{U}}_{k,p_k^*}$ ,  $k = \{1, \dots, K\}$ , to the remaining weaker BCUs via the common bus. Thus, matrix  $\mathbf{D} = \text{Blkdiag}\{\tilde{\mathbf{U}}_{1,p_1^*} \dots \tilde{\mathbf{U}}_{K,p_K^*}\}$  and the local Gram matrix  $\mathbf{G}_p$  in (6) can be obtained at BCU  $p$ ,  $\forall p$ . Then, the BCUs share the local Gram matrices  $\mathbf{G}_p$ , compute the aggregate Gram matrix  $\mathbf{G}$  in (6), and calculate the local precoding matrix  $\mathbf{W}_p$  in (7), for  $p = \{1, \dots, P\}$ . Finally, the locally precoded signal vector at BCU  $p$ ,  $\forall p$ , can be obtained as follows:

$$\mathbf{x}_p = \mathbf{W}_p \mathbf{s}, \quad \forall p, \quad (9)$$

and is forwarded from the *Precoder* blocks to the RF chains via the *internal bus* for downlink transmission, see Fig. 2.

In contrast to the centralized EZF precoding scheme in Section II-B and the DEZF approach in [14], where the CPU node computes an SVD for  $K$  channel matrices, in our scheme, only the *strongest* BCU computes the SVD of the local channel matrix of a given user. Thus, the computational burden of the CPU node of the approach in [7], [14] is distributed across different BCUs in the proposed APD EZF scheme. Furthermore, the dimensionality of the local channel matrices at one BCU depends only on the number of antennas per BCU  $M$  and not on the total number of BS antennas  $N_{\text{T}} \geq M$ . Hence, we conclude that the computational complexity required at one BCU of the proposed scheme is lower compared to the complexity required at the CPU node of the scheme in [7], [14].

## IV. FRONTHAUL LOAD AND PERFORMANCE ANALYSIS

In this section, we numerically investigate the fronthaul load and MU-MIMO system performance of the proposed APD EZF precoding scheme for the distributed BS design in Fig. 2.

### A. Fronthaul Load Analysis

In the following, we numerically evaluate the fronthaul load of the proposed distributed precoding scheme and compare it with the fronthaul load of the centralized EZF approach in [7] and the DEZF scheme in [14]. Let us first denote the fronthaul loads of the centralized EZF, the DEZF, and the proposed APD EZF schemes by  $\zeta_{\text{CEN}}$ ,  $\zeta_{\text{DEZF}}$ , and  $\zeta_{\text{APD}}$ , respectively, which are expressed in terms of the number of real values exchanged via the *fronthaul bus* at the BS. Then, the relative fronthaul load gain achieved by the APD EZF and DEZF schemes compared to the baseline EZF scheme is given by  $\hat{\zeta}_X = 1 - (\zeta_X / \zeta_{\text{CEN}})$ , for  $X = \{\text{APD}, \text{DEZF}\}$ .

In the centralized EZF scheme, for the computation of the precoder matrix  $\mathbf{W}$ , no information is exchanged between the CPU and the RF chains at the BS, given that the precoder is computed

TABLE I: Fronthaul load gain of the APD EZF and DEZF schemes, for varying system load  $\eta$ .

System Parameters	$M = 64$	$P = 4$	$L = 2$	$N_R = 4$	$\tau = 65$
Fronthaul load gain					
$K, \eta$	$\hat{\zeta}_{\text{APD}}$ (proposed)		$\hat{\zeta}_{\text{DEZF}}$		
$K = 16, \eta = 12.50\%$	74.33%		68.27%		
$K = 24, \eta = 18.75\%$	52.26%		40.87%		
$K = 32, \eta = 25.00\%$	24.04%		5.77%		
$K = 36, \eta = 28.125\%$	7.62%		-14.66%		

TABLE II: Fronthaul load gain of the APD EZF and DEZF schemes, for varying number of BCUs  $P$ .

System Parameters	$N_T = 256$	$K = 16$	$L = 2$	$N_R = 4$	$\tau = 65$
Fronthaul load gain					
$P, M$	$\hat{\zeta}_{\text{APD}}$ (proposed)		$\hat{\zeta}_{\text{DEZF}}$		
$P = 4, M = 64$	74.33%		68.27%		
$P = 8, M = 32$	61.83%		52.88%		
$P = 16, M = 16$	36.83%		22.12%		

in a centralized manner at the CPU. For a typical scenario, where the channel is static across  $\tau$  consecutive symbol intervals, the only information that is exchanged between the CPU and the RF chains for each symbol interval is the complex valued precoded signal vector  $\mathbf{x}$ , see also Fig. 1. Thus, the resulting fronthaul load is  $\zeta_{\text{CEN}} = 2\tau N_T$ . Meanwhile, in the proposed the APD scheme, the information shared between BCUs comprises symbol vector  $\mathbf{s}$ , metrics  $\mathcal{T}_{k,p}$ , and matrices  $\tilde{\mathbf{U}}_{k,p}^*$  and  $\mathbf{G}_p$ , respectively, which results in  $\zeta_{\text{APD}} = PK + 2L_{\text{tot}}N_R - L_{\text{tot}} + PL_{\text{tot}}^2 + 2\tau L_{\text{tot}}$ . Lastly, the fronthaul load of the DEZF scheme,  $\zeta_{\text{DEZF}}$ , is computed as in [14].

Next, we define the system load  $\eta$  as the ratio between the total number of transmit data streams,  $L_{\text{tot}}$ , and the total number of transmit antennas at the BS,  $N_T$ , i.e.,  $\eta = L_{\text{tot}}/N_T$ . To analyze the impact of  $\eta$  on the fronthaul load gain of the APD EZF and DEZF schemes, we fix the remaining system parameters, see Table I. From the results shown in Table I, we observe that the proposed APD EZF scheme outperforms both the centralized EZF and the DEZF approach in terms of fronthaul complexity requirements, i.e.,  $\hat{\zeta}_{\text{APD}} > 0$  and  $\hat{\zeta}_{\text{APD}} > \hat{\zeta}_{\text{DEZF}}$ , respectively, for all considered cases. In particular, for  $\eta = 12.5\%$ , the APD EZF scheme achieves a gain of 74.33% compared to centralized EZF, nearly 6% more than the gain achieved by the DEZF approach. Furthermore, as the system load increases, the gap between the APD EZF and the DEZF schemes becomes more significant, exceeding 20% for  $K = 36$ . Additionally, for  $K = 36$ , in contrast to our proposed scheme, which yields a positive gain of 7.62%, DEZF exceeds the fronthaul load of centralized EZF, i.e.,  $\hat{\zeta}_{\text{DEZF}} < 0$ . Finally, we note that an increase of the system load leads to lower fronthaul load gains compared to centralized EZF for both the APD EZF and the DEZF schemes given that their fronthaul loads depend on the total number of users  $K$ .

Next, we consider the impact of the number of antennas per BCU,  $M$ , on the fronthaul load gain  $\hat{\zeta}_\chi$ ,  $\forall \chi$ . Similar to the analysis conducted with respect to  $\eta$ , we fix the remaining system parameters and vary  $M$ . As the results given in Table II show, the proposed APD EZF scheme entails a lower fronthaul load compared to centralized EZF and DEZF, i.e.,  $\hat{\zeta}_{\text{APD}} > 0$  and  $\hat{\zeta}_{\text{APD}} > \hat{\zeta}_{\text{DEZF}}$ , respectively, for all considered scenarios. Furthermore, the benefits of the APD EZF scheme over the DEZF

approach become more prominent as the number of antennas per BCU  $M$  decreases. In particular, for  $(P, M) = (16, 16)$ , our scheme outperforms DEZF by more than 14%. Although a lower  $M$ , i.e., higher number of BCUs  $P$  at the BS, enables a lower computational complexity per BCU, see Section III-B, it results in a higher fronthaul load for the APD EZF and DEZF approaches, i.e., we obtain lower  $\hat{\zeta}_\chi$ ,  $\forall \chi$ , see Table II. Thus, a more modular BS design, i.e., lower  $M$ , poses a trade-off between fronthaul load and computational complexity.

## B. Performance Analysis

In this section, we numerically evaluate the performance of the proposed precoding scheme. To obtain channel matrices  $\mathbf{H}_k$ ,  $\forall k$ , for realistic communication scenarios, we set the carrier frequency  $f_c$  to 2.1 GHz and model the communication environment using QuaDRiGa [16]. The BCUs at the BS are modeled as uniform planar arrays (UPAs) with cross-polarized antennas. The spacing between any two adjacent antenna elements at the BS is set to  $0.5\lambda$ , where  $\lambda = \frac{c}{f_c}$  is the wavelength and  $c$  is the speed of light. The users are placed randomly in a  $120^\circ$  sector in a range of 50 m-120 m from the BS and are equipped with  $N_R \times 1$  vertical uniform linear arrays (ULAs) with omnidirectional antennas. The transmit symbols are chosen from a 16-ary quadrature amplitude modulation (16-QAM) constellation. Throughout this section, the number of antennas at the BS is  $N_T = 256$ , the number of streams per user is  $L = 2$ , and the number of antennas per user equals  $N_R = 4$ .

In the following, we compare the uncoded bit-error rates (BERs) obtained for the proposed APD EZF scheme with the corresponding results for the centralized EZF/DEZF [7], [14] and the FD EZF [9] schemes, respectively. For the FD EZF scheme, we optimistically assume that the equalization vectors  $\mathbf{u}_{k,l}$ ,  $\forall k, l$ , are known to all the BCUs, and BCU  $p$  computes the local precoding vector of data stream  $i$  as  $\mathbf{w}_{p,i} = \frac{\hat{\mathbf{c}}_{p,i}}{\|\hat{\mathbf{c}}_{p,i}\|\sqrt{P}}$ , where  $\hat{\mathbf{c}}_{p,i}$  is the  $i$ th column of  $\mathbf{C}_p^\dagger$ ,  $\forall p, i$ , [9].

To analyze the impact of the number of antennas per BCU  $M$  on the uncoded BER of the proposed APD EZF scheme, we fix the number of users to  $K = 16$ , and consider  $(P, M) = \{(4, 64), (8, 32)\}$ . As the results in Fig. 3 show, the proposed APD EZF scheme achieves almost the same performance as centralized EZF and DEZF, for all considered cases. Furthermore, the APD EZF approach significantly outperforms the FD EZF scheme for all considered  $(P, M)$  combinations. For the FD EZF scheme, we still serve all  $K$  users, but local EZF based on  $M \leq N_T$  BS antennas instead of  $N_T$  antennas is performed [9], and therefore, a decrease of  $M$  has a detrimental effect on the performance of the FD EZF scheme. For example, for  $(P, M) = (4, 64)$ , the FD EZF scheme experiences a loss of approximately 9 dB in combining gain compared to the APD EZF scheme, and the loss increases further to nearly 30 dB for  $(P, M) = (8, 32)$ . In contrast, a more modular BS architecture, i.e., smaller  $M$  and larger  $P$ , does not compromise the performance of the proposed APD EZF approach.

Next, we study the impact of the system load  $\eta$  on the BER performance of the proposed APD EZF scheme for  $P = 4$  and  $K = \{32, 64\}$ , i.e.,  $\eta = \{25\%, 50\%\}$ . As the results depicted

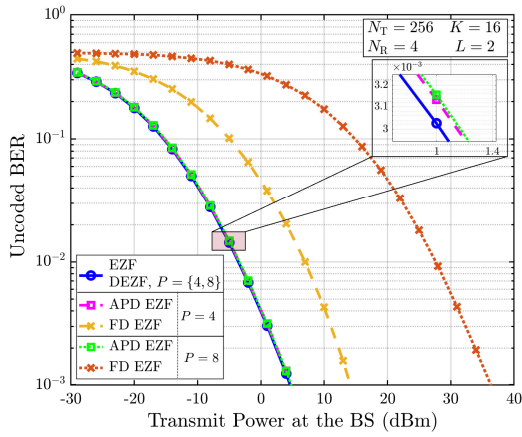


Fig. 3: Uncoded BER versus transmit power at the BS for varying number of BCUs  $P$ .

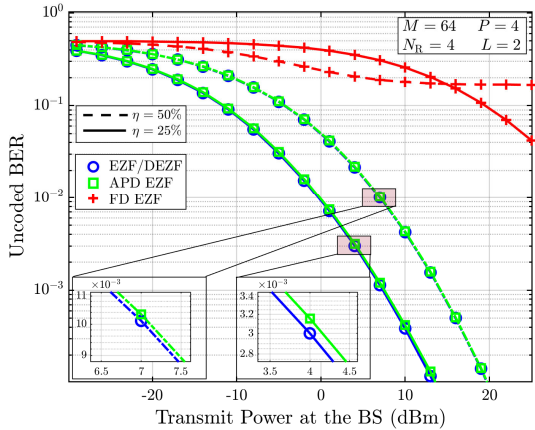


Fig. 4: Uncoded BER versus transmit power at the BS for varying system load  $\eta$ .

in Fig. 4 show, there is almost no gap between the BER for the proposed APD EZF and the centralized EZF and DEZF schemes, for all considered values of  $\eta$ . Furthermore, the proposed scheme significantly outperforms the FD approach. In fact, in contrast to the proposed approach, the FD EZF scheme is not able to cancel the inter-user-interference (IUI) for  $\eta = 50\%$  since  $M < L_{\text{tot}}$ , which leads to an error floor.

For both of the cases considered above, i.e., higher  $\eta$  and  $P$ , respectively, the proposed APD EZF scheme still performs channel inversion for perfect IUI cancellation. Nevertheless, APD EZF does not perform beam steering using the strongest eigenchannels for each user. Instead, it selects sub-optimal channels based only on the eigenbeams of the local CSI of the *strongest* BCU. As the BER curves in Fig. 3 and Fig. 4 indicate, the *strongest* BCU is capable of selecting close-to-optimal channels for  $M > L$ , resulting in only a negligible performance loss compared to the centralized EZF/DEZF schemes.

## V. CONCLUSIONS

In this paper, we have proposed a novel approach for distributed BS signal processing in massive downlink multiple-antenna MU-MIMO systems, where each user device is simultaneously served with multiple data streams. We have proposed a novel decentralized BS architecture which does not rely on a

CPU node for centralized baseband signal processing. Instead, it distributes the computational complexity burden of the baseband signal processing tasks across different clusters of BS antennas. Next, for the proposed BS architecture, we have developed a novel decentralized precoding algorithm based on linear EZF. Our numerical simulations showed that the proposed APD EZF scheme can achieve a significantly lower fronthaul load compared to the baseline centralized EZF and DEZF schemes, for various numbers of BS antenna clusters and different values of system load. Furthermore, we have shown that the APD EZF scheme achieves nearly the same BER performance as the considered baseline EZF and DEZF schemes and it outperforms the FD EZF approach for different system setups.

## REFERENCES

- [1] F. Rusek, D. Persson, B. K. Lau, E. G. Larsson, T. L. Marzetta, O. Edfors, and F. Tufvesson, "Scaling up MIMO: Opportunities and Challenges with Very Large Arrays," *IEEE Signal Process. Mag.*, vol. 30, no. 1, pp. 40–60, 2013.
- [2] L. Lu, G. Y. Li, A. L. Swindlehurst, A. Ashikhmin, and R. Zhang, "An Overview of Massive MIMO: Benefits and Challenges," *IEEE J. Sel. Topics Signal Process.*, vol. 8, no. 5, pp. 742–758, 2014.
- [3] H. Papadopoulos, C. Wang, O. Bursalioglu, X. How, and Y. Kishiyama, "MIMO Technologies and Challenges towards 5G," *IEICE Trans. Commun.*, vol. E99-B, Mar. 2016.
- [4] E. Björnson, E. G. Larsson, and T. L. Marzetta, "Massive MIMO: Ten Myths and One Critical Question," *IEEE Commun. Mag.*, vol. 54, no. 2, pp. 114–123, 2016.
- [5] H. Yang and T. L. Marzetta, "Performance of Conjugate and Zero-Forcing Beamforming in Large-Scale Antenna Systems," *IEEE J. Sel. Areas Commun.*, vol. 31, no. 2, pp. 172–179, 2013.
- [6] J. Hoydis, S. ten Brink, and M. Debbah, "Massive MIMO in the UL/DL of Cellular Networks: How Many Antennas Do We Need?" *IEEE J. Sel. Areas Commun.*, vol. 31, no. 2, pp. 160–171, 2013.
- [7] L. Sun and M. R. McKay, "Eigen-Based Transceivers for the MIMO Broadcast Channel with Semi-Orthogonal User Selection," *IEEE Trans. Signal Process.*, vol. 58, no. 10, pp. 5246–5261, Oct. 2010.
- [8] K. Li, R. R. Sharan, Y. Chen, T. Goldstein, J. R. Cavallaro, and C. Studer, "Decentralized Baseband Processing for Massive MU-MIMO Systems," *IEEE J. Emerg. Sel. Topics Circuits Syst.*, vol. 7, no. 4, pp. 491–507, Dec. 2017.
- [9] K. Li, C. Jeon, J. R. Cavallaro, and C. Studer, "Feedforward Architectures for Decentralized Precoding in Massive MU-MIMO Systems," in *Proc. 52nd Asilomar Conf. Signals, Syst., Comput.*, pp. 1659–1665, Oct. 2018.
- [10] K. Li, O. Castaneda, C. Jeon, J. R. Cavallaro, and C. Studer, "Decentralized Coordinate-Descent Data Detection and Precoding for Massive MU-MIMO," in *Proc. IEEE Int. Symp. on Circuits and Syst. (ISCAS)*, May 2019.
- [11] M. Liu, F. Sarajlic, J. Rusek, R. L. Sanchez, and O. Edfors, "Fully Decentralized Approximate Zero-Forcing Precoding for Massive MIMO Systems," *IEEE Wireless Commun. Lett.*, vol. 8, no. 3, pp. 773–776, Jun. 2019.
- [12] J. R. Sanchez, F. Rusek, O. Edfors, M. Sarajlic, and L. Liu, "Decentralized Massive MIMO Processing Exploring Daisy-Chain Architecture and Recursive Algorithms," *IEEE Trans. Signal Process.*, vol. 68, pp. 687–700, 2020.
- [13] K. Li, J. McNaney, C. Tarver, O. Castaneda, C. Jeon, J. R. Cavallaro, and C. Studer, "Design Trade-offs for Decentralized Baseband Processing in Massive MU-MIMO Systems," in *Proc. 53rd Asilomar Conf. on Signals, Syst., and Comput.*, pp. 906–912, 2019.
- [14] X. Zhao, M. Li, Y. Liu, T.-H. Chang, and Q. Shi, "Communication-Efficient Decentralized Linear Precoding for Massive MU-MIMO Systems," *IEEE Trans. Signal Process.*, vol. 71, pp. 4045–4059, 2023.
- [15] R. G. Horn and C. A. Johnson, *Matrix Analysis*. Cambridge, U.K.: Cambridge Univ. Press, 1985.
- [16] S. Jaeckel, L. Raschkowski, K. Boerner, L. Thiele, F. Burkhardt, and E. Eberlein, "QuaDRiGa - Quasi Deterministic Radio Channel Generator, User Manual and Documentation," *Fraunhofer Heinrich Hertz Institute, Tech. Rep.*, vol. v2.6.1, 2021.